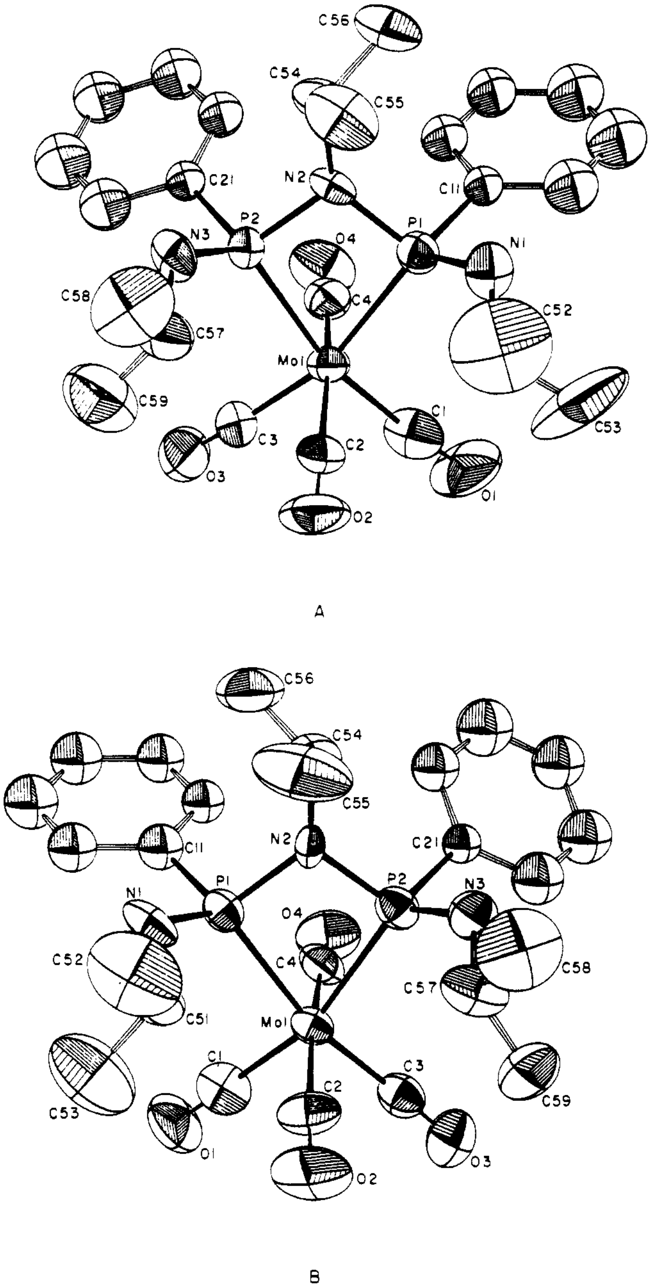

Figure 1. ORTEP drawing and numbering scheme for *cis-meso-i*-PrN-[PhP(*i*-PrNH)]$_2$Mo(CO)$_4$ (**4**) showing 50% probability ellipsoids of all atoms. Hydrogen atoms are omitted for clarity. Selected bond lengths (Å) and angles (deg), mean for molecules A and B: Mo–P(1), 2.497 (5); Mo–P(2), 2.492 (5); P(1)–N(2), 1.72 (1); P(2)–N(2), 1.69 (1); P(2)–N(3), 1.68 (2); P(1)–N(1), 1.68 (2); P(1)–C(11), 1.83 (1); P(2)–C(21), 1.82 (1); N(2)–C(54), 1.49 (2); P(1)–Mo–P(2), 65.1 (2); P(1)–N(2)–P(2), 104.3 (8); N(2)–P(1)–Mo, 94.9 (5); N(2)–P(2)–Mo, 95.8 (4); Mo–P(1)–N(1), 124.1 (6); Mo–P(2)–N(3), 126.5 (5); P(2)–Mo–C(3), 99.4 (7); P(2)–Mo–C(1), 165.5 (6); Mo–P(1)–C(11), 119.5 (4); Mo–P(2)–C(21), 118.7 (4); N(1)–P(1)–C(11), 100.5 (7); N(3)–P(2)–C(21), 106.3 (6); N(2)–P(1)–N(1), 111.4 (7); N(2)–P(2)–N(3), 110.5 (7); P(1)–Mo–C(1), 100.5 (6); P(1)–Mo–C(4), 92.0 (6); P(2)–Mo–C(2), 97.8 (6); P(2)–Mo–C(4), 88.7 (6); P(1)–Mo–C(2), 99.9 (6); P(1)–Mo–C(3), 163.5 (7).

The origin of diastereomer formation selectivity in the *i*-PrNH$_2$–PhPCl$_2$ reaction and the extent to which this is general in RNH$_2$–R′PCl$_2$ reactions or other diphosphinoamine formation reactions is unclear. Aniline and PhPCl$_2$ react at 25 °C to form both *d,l* and meso products.[16] Previous studies of MeN[P(NMe$_2$)$_2$]$_2$–PCl$_3$ and MeN(SiMe$_3$)$_2$–MePCl$_2$ reactions yield MeN[P(Cl)NMe$_2$]$_2$ and MeN[P(NMe)(Cl)SiMe$_3$]$_2$, respectively, which were suggested but not proved to be monodiastereomers.[6,10] In some cases, single-diastereomer product formation could have occurred but because the products were isolated by distillation at elevated temperatures product isomerization might be expected. *meso*-**3** does not form through *i*-PrNH$_2$ elimination between molecules of **2**; **3** forms only slowly as a *d,l*-meso mixture from **2** at 130 °C.

Diastereomer selection likely occurs because of conformation selection (excess population of one rotomer) in either intermediate or transition-state P–Cl bond-containing species. It is possible that, through variations in substitution and/or through use of other diphosphinoamine formation reactions, ways will be found to control diastereomer formation so that either meso or *d,l* isomers can be selectively formed. Such reactions are being studied currently in our laboratories.

Acknowledgment. Support for this work from National Science Foundation Grant CHE 8312856 is gratefully acknowledged.

Registry No. **2**, 716-85-8; **3**, 98087-84-4; **4**, 98087-85-5; *i*-PrNH$_2$, 75-31-0; PhPCl$_2$, 644-97-3; (norbornadiene)tetracarbonylmolybdenum, 12146-37-1.

Supplementary Material Available: Listings of details of the crystal structure determination and crystal structure data, positional parameters, anisotropic thermal parameters, bond distances, and bond angles (10 pages). Ordering information is given on any current masthead page.

Department of Chemistry
University of Colorado
Boulder, Colorado 80309

Tara G. Hill
R. Curtis Haltiwanger
Arlan D. Norman*

Received April 25, 1985

---

[16] Hill, T. G. Ph.D. Thesis, University of Colorado, 1985.

[17] Keat, R. *Top. Curr. Chem.* **1982**, *102*, 89.

Role of the Intermolecular Interactions in the Two-Dimensional Ambient-Pressure Organic Superconductors β-(ET)$_2$I$_3$ and β-(ET)$_2$IBr$_2$

Sir:

Two ambient-pressure organic superconductors have recently been synthesized from the sulfur-containing organic donor bis(ethylenedithio)tetrathiafulvalene (BEDT-TTF or ET, **1**).[1-9]

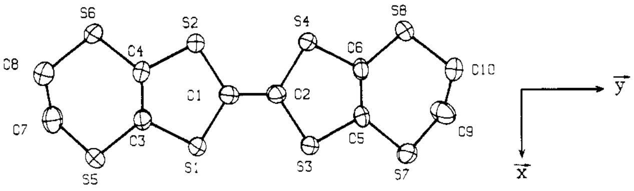

1

---

[1] Yagubskii, E. B.; Shchegolev, I. F.; Laukhin, V. N.; Kononovich, P. A.; Kartsovnik, M. V.; Zvarykina, A. V.; Buravov, L. I. *Pis'ma Zh. Eksp. Teor. Fiz.* **1984**, *39*, 12; *JETP Lett.* (*Engl. Transl.*) **1984**, *39*, 12.

[2] Crabtree, G. W.; Carlson, K. D.; Hall, L. N.; Copps, P. T.; Wang, H. H.; Emge, T. J.; Beno, M. A.; Williams, J. M. *Phys. Rev. B: Condens. Matter* **1984**, *30*, 2958.

[3] Williams, J. M.; Emge, T. J.; Wang, H. H.; Beno, M. A.; Copps, P. T.; Hall, L. N.; Carlson, K. D.; Crabtree, G. W. *Inorg. Chem.* **1984**, *23*, 2558.

[4] Carlson, K. D.; Crabtree, G. W.; Choi, M.; Hall, L. N.; Copps, P. T.; Wang, H. H.; Emge, T. J.; Beno, M. A.; Williams, J. M. *Mol. Cryst. Liq. Cryst.* **1985**, *125*, 145.

[5] Azevedo, L. J.; Venturini, E. L.; Schirber, J. E.; Williams, J. M.; Wang, H. H.; Emge, T. J. *Mol. Cryst. Liq. Cryt.* **1985**, *119*, 389.

[6] Hennig, I.; Bender, K.; Schweitzer, D.; Dietz, K.; Endres, H.; Keller, H. J.; Gleitz, A.; Helberg, H. W. *Mol. Cryst. Liq. Cryst.* **1985**, *119*, 337.

[7] Schwenk, H.; Gross, F.; Heidmann, C. P.; Andres, K.; Schweitzer, D.; Keller, H. *Mol. Cryst. Liq. Cryst.* **1985**, *119*, 329.

[8] Williams, J. M.; Wang, H. H.; Beno, M. A.; Emge, T. J.; Sowa, L. M.; Copps, P. T.; Behroozi, F.; Hall, L. N.; Carlson, K. D.; Crabtree, G. W. *Inorg. Chem.* **1984**, *23*, 3839.

[9] Mortensen, K.; Jacobsen, C. S.; Bechgaard, K.; Carneiro, K.; Williams, J. M. *Mol. Cryst. Liq. Cryst.* **1985**, *119*, 401.

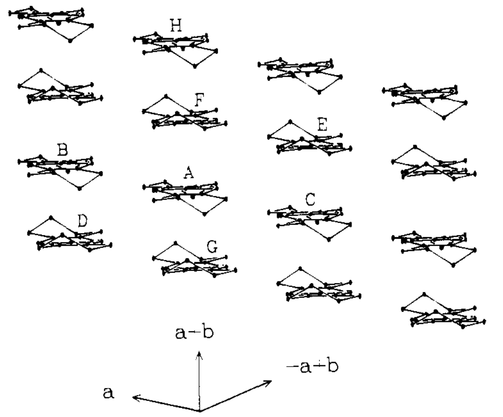

Figure 1. Illustration of the packing of the ET molecules in β-$(ET)_2I_3$ and β-$(ET)_2IBr_2$.[3,8] The perspective view is along the molecular axes. The projections of the unit cell axes are indicated.

These superconductors β-$(ET)_2I_3$ ($T_c \simeq 1.6$ K)[2-7] and β-$(ET)_2IBr_2$ ($T_c \simeq 2.8$ K)[8] have stacks of ET molecules, and each ET stack contains loosely dimerized $(ET)_2^+$ units that repeat along the $a + b$ direction. The ET stacks also form molecular sheets parallel to the ab plane, as depicted in Figure 1.[3,8] In the β-$(ET)_2X$ crystals, the sheets of $(ET)_2^+$ dimers and X^- anions (I_3^- or IBr_2^-) alternate along the c direction. Between adjacent ET stacks in each ET sheet, numerous short S···S contact distances less than 3.6 Å(i.e., the van der Waals radii sum of the S atoms) occur along the directions a and $-a + b$, which suggests the presence of strong interstack interactions. In agreement with these structural characteristics, various electrical conductivity[2,4,5,7-9] and optical[11] measurements and band electronic structure calculations[12,13] reveal that the β-$(ET)_2X$ salts are two-dimensional (2D) metals.

In the following, we examine the intermolecular interactions between the ET molecules and their relations to the band structure. In order to better describe the interstack S···S interactions, the s and p orbitals of carbon and sulfur were represented by double-ζ Slater type orbitals[14] as employed in our band electronic structure calculations.[13] Also, the significance of the short interstack S···S contacts for the interactions between ET molecules will be examined.

As shown in Figure 1, an ET molecule (e.g. A) has six nearest-neighbor ET molecules (e.g. B through G) within each ET sheet. It is important to distinguish the two kinds of sulfur atoms in the ET molecule: the four inner sulfur atoms of the TTF moiety (S_i) and the outer sulfur atoms of the two ethylenedithio bridges (S_o). Thus for each of the six nearest-neighbor ET pairs (i–j), where i = A and j = B through G (see Figure 1), there occur three types of S···S contacts, i.e., $S_i \cdots S_i$, $S_i \cdots S_o$, and $S_o \cdots S_o$, respectively. In the present study, the interaction energies[14] $\beta_{ij} = \langle \psi_i | H^{\text{eff}} | \psi_j \rangle$ between the HOMO's ψ_i and ψ_j calculated for the six nearest-neighbor ET pairs (i–j) are found to be related to the packing geometries and are determined primarily by the $S_i \cdots S_i$ interactions.

Table I. Geometrical Parameters (Δy, R, ϕ) and Interaction Energies (β_{ij}) of the ET Pairs in β-$(ET)_2I_3$ and β-$(ET)_2IBr_2$

A. Interaction Energies β_{ij} (eV)

	β-$(ET)_2I_3$		β-$(ET)_2IBr_2$	
pair (i–j)	298 K	120 K[a]	298 K	120 K
(A–B)[b]	0.017	0.011	0.022	0.012
(A–E)	0.156	0.158	0.148	0.167
(A–F)	0.266	0.304	0.325	0.325
(A–G)	0.423	0.474	0.463	0.490
$W_\parallel$[c]	0.532	0.608	0.650	0.650
$W_\perp$	0.504	0.488	0.514	0.532

B. Geometrical Parameters Δy (Å), R (Å), and Φ (deg)[d]

pair (i–j)	Δy	R	ϕ
(A–B)	−1.83	6.36	−13.5
(A–D)	−0.17	6.53	16.9
(A–E)	−2.13	6.27	23.4
(A–F)	−3.96	4.00	−83.9
(A–G)	1.66	3.39	88.8

[a] This material undergoes an incommensurate structural modulation at ~195 K (see ref 18). The calculations are based on the "average" structure. [b] By symmetry, the A–B and A–C pairs are identical. [c] $W_\parallel$ and $W_\perp$ are the estimated band widths along the intrastack and interstack directions. [d] The geometrical parameters are taken from the crystal structure of β-$(ET)_2I_3$ at 298 K.[3]

With a formal charge of +0.5 electron per ET molecule, there are three valence electrons in the HOMO's for the two ET molecules per unit cell. The interstack and intrastack interactions of the ET molecules lead to two split bands, characterized by bonding and antibonding combinations of the HOMO's of two ET molecules in each unit cell.[13] Thus, the valence band structure is composed of a completely filled lower band and a half-filled upper band.[13] Listed in Table I are the β_{ij} values for the crystal structures of β-$(ET)_2I_3$ and β-$(ET)_2IBr_2$ at 298 and 120 K. All of the β_{ij} values are positive since all of the overlap integrals $\langle \psi_i | \psi_j \rangle$ are negative when the phases of the HOMO's ψ_i and ψ_j are taken to be the same. Along the stacking direction $a + b$, there exist two different nearest-neighbor interactions (A–F) and (A–G), with interaction energies β_{A-F} and β_{A-G}, respectively. Since $\beta_{A-F} < \beta_{A-G}$, the width of the valence band along the stacking direction is approximately given by $W_\parallel \simeq 2\beta_{A-F} = 0.53$ eV.[15] Along the interstack directions a and $-a + b$, there occur four interactions[16] per ET molecule, with the average interaction energy $\beta_{av} = (\beta_{A-B} + \beta_{A-C} + \beta_{A-D} + \beta_{A-E})/2 = 0.126$ eV per ET. The width of the valence band along the interstack direction is approximately given by $W_\perp \simeq 4\beta_{av} = 0.50$ eV.[15] Thus the valence band based on the pairwise interactions is nearly isotropic in two dimensions (i.e., $W_\perp \simeq W_\parallel$), in good agreement with our previous band structure calculations.[13]

Let us now examine how the magnitudes of the β_{ij} values may be related to the S···S contact distances. The shortest S···S distances observed for each of the $S_i \cdots S_i$, $S_i \cdots S_o$, and $S_o \cdots S_o$ interactions have been previously analyzed in terms of the six (i–j) pairs of ET molecules.[3,8] Important structural features that characterize an (i–j) molecular pair are their relative orientations[17] (**2**), where $R = [(\Delta x)^2 + (\Delta z)^2]^{1/2}$ and $\phi = \tan^{-1}(\Delta z/\Delta x)$ and where the displacement of molecule j with respect to i is (Δx, Δy, Δz) in the Cartesian system (see **1**). The Δy, R, and ϕ values for the six (i–j) pairs in β-$(ET)_2I_3$ at 298 K are listed in Table I. We observe that the S···S distances less than ~3.6 Å occur between the interstack pairs (A–B), (A–C), (A–D) and (A–E), which all

---

(10) Kaminskii, V. F.; Prokhorova, T. G.; Shibaeva, R. P.; Yagubskii, E. B. *Pis'ma Zh. Eksp. Teor. Fiz.* **1984**, *39*, 15; *JETP Lett.* (*Engl. Transl.*) **1984**, *39*, 17.

(11) Jacobsen, C. S.; Williams, J. M.; Wang, H. H. *Solid State Commun.* **1985**, *54*, 937.

(12) Mori, T.; Kobayashi, A.; Sasaki, Y.; Kobyashi, H.; Saito, G.; Inokuchi, H. *Chem. Lett.* **1984**, 957.

(13) Whangbo, M.-H.; Williams, J. M.; Leung, P. C. W.; Beno, M. A.; Emge, T. J.; Wang, H. H.; Crabtree, G. W.; Carlson, K. D. *J. Am. Chem. Soc.*, in press.

(14) (a) In the present work, the interaction energies β_{ij} were calculated by employing the extended Hückel method (Hoffmann, R. *J. Chem. Phys.* **1963**, *39*, 1397). For sulfur and carbon, each atomic orbital was represented by a linear combination of two Slater-type orbitals of exponents ζ_μ and ζ_μ' with the weighting coefficients c_μ and c_μ', respectively (Clementi, E.; Roetti, C. *At. Data Nucl. Data Tables* **1974**, *14*, 177). The ζ_μ, ζ_μ', c_μ, c_μ' and $H_{\mu\mu}$ (valence shell ionization potential) values employed in our study are respectively 2.662, 1.688, 0.5564, 0.4874, −20.0 eV for S 3s; 2.338, 1.333, 0.5212, 0.5443, −13.3 eV for S 3p; 1.831, 1.153, 0.7616, 0.2630, −21.4 eV for C 2s; 2.730, 1.257, 0.2595, 0.8025, −11.4 eV for C 2p. A modified Wolfsberg–Helmholz formula was used to calculate $H_{\mu\nu}$ (Ammeter, J. H.; Bürgi, H. B.; Thibeault, J. C.; Hoffmann, R. *J. Am. Chem. Soc.* **1978**, *100*, 3686). (b) Grant, P. M. *Phys. Rev B: Condens. Matter* **1983**, *27*, 3934.

(15) Albright, T. A.; Burdett, J. K.; Whangbo, M.-H. "Orbital Interactions in Chemistry"; Wiley: New York, 1985; Chapter 13.

(16) To correctly count the various (i–j) interactions, a unit cell may be chosen as A + (F + G)/2 in the notations of Figure 1.

(17) Mori, T.; Kobayashi, A.; Sasaki, Y.; Kobayashi, H.; Saito, G.; Inokuchi, H. *Bull. Chem. Soc. Jpn.* **1984**, *57*, 627.

(18) Leung, P. C. W.; Emge, T. J.; Beno, M. A.; Wang, H. H.; Williams, J. M.; Petricek, V.; Coppens, P. *J. Am. Chem. Soc.* **1984**, *106*, 7644.

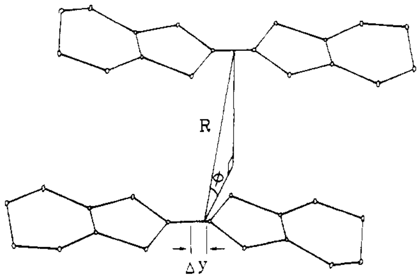

2

have *smaller* interaction energies than (A–F) and (A–G). Among the six possible pairs of interacting ET molecules (see Figure 1), the crystallographically equivalent A–B and A–C pairs have the smallest β_{ij} values, but these pairs contain most of the shortest S···S contact distances. However, the network of S···S distances in the *ab* plane contracts for *all* ET pairs when the IBr_2^- anion replaces the I_3^- anion or when the temperature is reduced (i.e., from 298 to 120 K). As a result of these contracted S···S distances, the intermolecular interactions β_{ij} and the estimated band widths $W_\parallel$ and $W_\perp$ increase systematically.[13]

While the intermolecular S···S distances are important, they are *not* the only measure of the extent of cation–cation interactions. The angle ϕ between the adjacent pair of ET molecules (Table I) is more important on the basis of geometric considerations. Since the HOMO is a π-type orbital, the ϕ values of 0 and 90° represent π- and σ-type interactions, respectively. For intermediate values, partial contributions from either π or σ occur and the net overlap may be positive or negative. The ϕ values for all six ET pairs are compared to the respective β_{ij} values in Table I.

Furthermore, the orbital coefficients of the HOMO of ET, as shown in **3**, reveal that the contribution of S_o is about 3 times smaller than that of S_i.

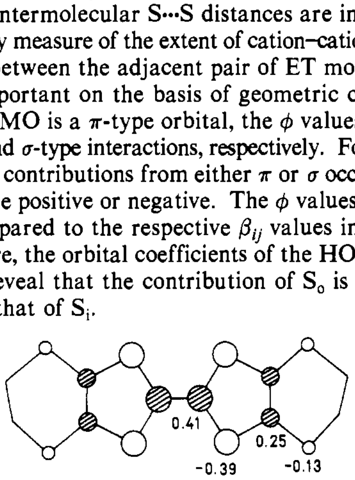

3

Since β_{ij} can be written as

$$\beta_{ij} = \sum_{\mu}\sum_{\nu} C_{\mu i}C_{\nu j}\langle\chi_\mu|H^{\mathrm{eff}}|\chi_\nu\rangle \qquad (1)$$

where $C_{\mu i}$ is the coefficient of the atomic orbital χ_μ in the HOMO ψ_i, the magnitudes of the S_o···S_o, S_i···S_o, and S_i···S_i interactions have the ratios 1:3:9 in terms of the weighting factors $C_{\mu i}C_{\nu j}$ alone. For these two reasons, the S_o···S_o and S_i···S_o contacts that are less than 3.6 Å do not contribute as significantly to β_{ij} and to the valence band as the S_i···S_i contacts do.

To summarize, the present calculations, which are based on the observed positions of the ET molecules in β-$(ET)_2I_3$ and β-$(ET)_2IBr_2$ obtained from X-ray diffraction experiments, indicate that the intermolecular interactions of the ET molecules *alone* are responsible for the 2D electrical properties. Both the intrastack *and* interstack interactions contribute to the band structure. Our results are consistent with previous findings[17] that the angle ϕ between the adjacent molecular planes of the ET molecules is an important geometric variable in describing the overlap integrals $\langle\psi_i|\psi_j\rangle$ and the interaction energies β_{ij}. While the S···S contacts may be of secondary importance, the S_i···S_i contacts are the most significant among them. The S_i···S_o and S_o···S_o contacts (<3.60 Å) are probably important in terms of crystal packing via core–core interactions and thereby affect the 2D interaction ET network and contribute to the electrical properties of these materials. The systematic comparison of the β_{ij} values in the four crystal structures described here suggests that the substitution of IBr_2^- for I_3^- has the same effect as temperature reduction. Thus, the intermolecular interactions in β-$(ET)_2IBr_2$ at 120 K are the strongest in this series of crystal structures, which suggests that this salt may be a better electrical conductor than β-$(ET)_2I_3$.

Acknowledgment. This work is in part supported by the Camille and Henry Dreyfus foundation through a Teacher-Scholar Award to M.-H.W. Work at Argonne National Laboratory is sponsored by the U.S. Department of Energy, Office of Basic Energy Sciences, Division of Material Sciences, under Contract W-31-109-ENG-38. We express our appreciation for computing time made available by the DOE on the ER-CRAY.

Registry No. β-$(ET)_2I_3$, 89061-05-2; β-$(ET)_2IBr_2$, 92671-95-9.

Supplementary Material Available: Tables of the packing geometries and interaction energies for β-$(ET)_2I_3$ and β-$(ET)_2IBr_2$ at 298 and 120 K (4 pages). Ordering information is given on any current masthead page.

Department of Chemistry
North Carolina State University
Raleigh, North Carolina 27650
Myung-Hwan Whangbo*

Chemistry and Materials Science and
Technology Divisions
Argonne National Laboratory
Argonne, Illinois 60439
Jack M. Williams*
Peter C. W. Leung
Mark A. Beno
Thomas J. Emge
Hau H. Wang

Received June 7, 1985

Reaction of Superoxide with Nitric Oxide to Form Peroxonitrite in Alkaline Aqueous Solution

Sir:

Although aqueous superoxide often acts as a one-electron reductant or less frequently as an oxidant, it rarely undergoes covalent bond formation with simple organic or inorganic compounds in water,[1,2] perhaps owing to its poor nucleophilicity in this solvent.[1] In this communication we show, however, that superoxide[3] can react with nitric oxide to form the peroxonitrite anion in deaerated aqueous solutions at pH 12–13:

$$O_2^- + NO = {}^-OONO \qquad (1)$$

This reaction represents one of the few examples[1a] of a radical–radical coupling of O_2^- with another odd-electron species to form a diamagnetic product. The reaction also may be of significance in natural waters[4] or prove useful for trapping and measuring low levels of superoxide in aqueous systems.

Peroxonitrite exhibits a broad absorption spectrum with a maximum at ca. 300 nm. Although stable for hours in 0.1 M base, at lower pH it rapidly protonates and subsequently rearranges to nitrate.[5] $^-OONO/HOONO$ is an intermediate in the reaction of hydrogen peroxide with nitrous acid[6] and in the alkaline autoxidation of hydroxylamine, chloramine, and nitrohydroxamate.[7] Halfpenny and Robinson[6b] reported that NO and H_2O_2 also react to form ^-OONO. However, under the conditions of this study, we found no evidence for this reaction.

Superoxide (15–200 μM) was prepared photochemically in a 1-cm quartz cuvette by the method of McDowell et al.,[8] with use

---

(1) (a) Sawyer, D. T.; Valentine, J. S. *Acc. Chem. Res.* **1981**, *14*, 393–400. (b) Fee, J. In "Metal Ion Activation of Dioxygen"; Spiro, T. G., Ed.; Wiley-Interscience: New York, 1980; pp 209–237.

(2) (a) Finkelstein, E.; Rosen, G. M.; Rauckman, E. J. *J. Am. Chem. Soc.* **1980**, *102*, 4994–4999. (b) Harbour, J. R.; Chow, V.; Bolton, J. R. *Can. J. Chem.* **1974**, *52*, 3549–3553.

(3) For simplicity, our use of "superoxide" or "O_2^-" refers to both O_2^- and its conjugate acid, the hydroperoxyl radical (HO_2), unless otherwise stated.

(4) Zafirious, O. C. In "Chemical Oceanography", 2nd ed.; Academic Press: New York, 1983; Vol. 8, pp 339–379.

(5) Hughes, M. N.; Nicklin, H. G. *J. Chem. Soc. A* **1968**, 450–452.

(6) (a) Gleu, K.; Hubold, R. *Z. Anorg. Chem.* **1935**, *223*, 305. (b) Halfpenny, E.; Robinson, P. L. *J. Chem. Soc.* **1952**, 928–938. (c) Anbar, M.; Taube, H. *J. Am. Chem. Soc.* **1954**, *76*, 6243–6247.

(7) (a) Anbar, M.; Yagil, G. *J. Am. Chem. Soc.* **1962**, *84*, 1790–1796. (b) Yagil, G.; Anbar, M. *J. Inorg. Nucl. Chem.* **1964**, *26*, 453–460 and references contained therein.

(8) McDowell, M. S.; Bakac, A.; Espenson, J. H. *Inorg. Chem.* **1983**, *22*, 847–848.

0020-1669/85/1324-3502$01.50/0